Add historical introduction
To be found in the complete version
of the book made in April with
Gregory

Find original

Corrected 30/11/13

Chapter 1

Preface

The elementary modes of nuclear excitation are vibrations and rotations, single–particle (quasiparticle) motion, and pairing vibrations and rotations. The specific reactions probing these modes are inelastic, single– and two– particle transfer processes respectively. Within this context one can posit that nuclear structure (bound) and reactions (continuum) are but two aspects of the same physics. This is the reason why they can be treated on equal footing in terms of elementary modes of excitation, within the framework of nuclear field theory (NFT). This theory provides the rules to diagonalize in a compact and economic way the nuclear Hamiltonian for both bound and continuum states correcting for overcompletness of the basis (particle–vibration coupling (structure), non–orthogonality (reaction)), and for Pauli principle violation.

Pairing vibrations and rotations, closely connected with nuclear superfluidity are, arguably, a paradigm of quantal nuclear phenomena. They thus play an important role within the field of nuclear structure. It is only natural that two–nucleon transfer plays a similar role concerning direct nuclear reactions. In fact, this is the central subject of the present monograph.

fermionic (quasi-)

At the basis of pairing phenomena one finds Cooper pairs, weakly bound, extended, strongly overlapping bosonic entities, made out of pairs of nucleons dressed by collective vibrations and interacting through the exchange of these vibrations as well as through the bare NN–interaction, eventually corrected by $3N$ contributions. Cooper pairs not only change the statistics of the nuclear stuff around the Fermi surface and, condensing, the properties of nuclei close to their ground state. They also display a rather remarkable mechanism of tunnelling between target and projectile in direct two–nucleon transfer reaction. In fact, being weakly bound ($\ll \epsilon_F$, Fermi energy) they display correlations over distances (correlation length) much larger than nuclear dimensions ($\gg R$, nuclear radius). On the other hand, Cooper pairs are forced to be confined within such dimensions by the action of the average potential, which can be viewed as an external field as far as these pairs are concerned.

The correlation length paradigm comes into evidence, for example, when two

nuclei are set into weak contact in a direct reaction. In this case, each of the partner nucleons of a Cooper pair has a finite probability to be confined within the mean field of each of the two nuclei. It is then natural that a Cooper pair can tunnel, equally well correlated, between target and projectile, through simultaneous than through successive transfer processes. Consequently, although one does not expects supercurrents in nuclei, one can study long–range pairing correlations in terms of individual quantal state. The above mentioned weak coupling Cooper pair tunnelling reminds the tunnelling mechanism of electronic Cooper pairs across a barrier (e.g. a dioxide layer) separating two superconductors, known as Josephson junction. The main difference is that, as a rule, in the nuclear time dependent junction ~~provided by a~~ direct two–nucleon transfer process, only one or even none of the two weakly interacting nuclei are superfluid (or superconducting). Now, in nuclei, paradigmatic example of fermionic finite many–body system, zero point fluctuations (ZPF) in general, and those associated with pair addition and pair substraction modes known as pairing vibrations in particular, are much stronger than in condensed matter. Consequently, and in keeping with the fact that pairing vibrations are the nuclear embodiment of Cooper pairs in nuclei, pairing correlations based on even a single Cooper pair can lead to clearly observable effects in two–nucleon transfer processes.

Nucleonic Cooper pair tunnelling has played and is playing a central role in the probing of these subtle quantal phenomena, both in the case of exotic nuclei as well as of nuclei lying along the stability valley, and have been instrumental in shedding light on the subject of pairing in nuclei at large, and on nuclear superfluidity in particular. Consequently, the subject of two–nucleon transfer occupies a central place in the present monograph both concerning the conceptual and the computational aspects of the description ~~on equal footing~~ of nuclear pairing, as well as regarding the quantitative confrontation of the results and predictions with the experimental findings.

Because the interweaving of the variety of elementary modes of nuclear excitation, the study of Cooper pair tunnelling in nuclei aside from requiring a consistent description of nuclear structure in terms of dressed quasiparticles and vibrations, resulting from both bare and induced interactions, involves also the description of one–nucleon transfer as well as knock out processes, ~~let alone inelastic and Coulomb excitation processes~~. The corresponding softwares COOPER, ONE, KNOCK, ~~INELASTIC and COULOMB~~ are briefly presented, referring to the web site for the corresponding files and input–output examples.

Summing up, general physical arguments and technical computational details, as well as the software used in the ~~descriptions and~~ calculation of ~~the~~ absolute two–nucleon transfer cross sections, making use of state of the art nuclear structure information, are provided. As a consequence, theoretical and experimental practitioners, as well as PhD students could use the present monograph at profit.

Concerning the notation, we have divided each chapter into sections. Each subsection may in turn be broken down into subsections. Equations and Figures are identified by the number of the chapter and that of the section. Thus (6.1.33)

labels the thirtythird equation of section 1 of chapter 6. Similarly, Fig. 6.1.2 labels the second figure of section 1 of chapter 6. Concerning the Appendices, they are labelled by the chapter number and by a Latin letter in alphabetical order, e.g. App. 6.A, App. 6.B, etc. Concerning equations and Figures, a sequential number is added. Thus (6.E.15) labels the fifteenth equation of Appendix E of chapter 6, while Fig. 6.F.1 labels the first figure of Appendix F of chapter 6.

Throughout, a number of footnotes are found. This is in keeping with the fact that footnotes can be useful. In particular they allow to emphasize relevant issues in an economic way. Being outside the main text, they allow to state eventual important results, without the need of elaborating on the proof. Within this context, cf. (Born, 1926), paper introducing the interpretation of the wavefunction squared as a probability, in a footnote. Most of the material contained in this monograph have been the subject of lectures of the four year course "Nuclear Structure Theory" which RAB delivered at the Department of Physics of the University of Milan, as well as at the Niels Bohr Institute and at Stony Brook (State University of New York). It was also presented by the authors in the course Nuclear Reactions held at the PhD School of Physics of the University of Milan.

Bibliography References

M. Born. Zur Quantenmechanik der Stoßvorgänge. *Zeitschr. f. Phys.*, 37:863, 1926.

Born, M. 1926 Zur ..... Zeitschr. f. Phys., 37:863

Modo de tener references en orden alfabetico (ver. p. 58 versión corregida 23/11/13

Gregory Potel Livermore, ..

Ricardo A. Broglia Milan

Version 24/11/13

Corrected 30/11/2013

Chapter 6

One–particle transfer

In what follows we present a derivation of the one–particle transfer differential cross section within the framework of the distoted wave Born approximation (DWBA) (cf. Satchler (1980); Broglia and Winther (2004) and refs. therein). The structure input for the calculations are mean field potentials and single–particle states dressed, within the formalism of Nuclear Field Theory, through the coupling with the variety of collective, (quasi–) bosonic vibrations, leading to modified formfactors[1] resulting from the interweaving of these vibrations and a number of orbitals with the original, unperturbed single–particle states (Bohr and Mottelson, 1975; Bès et al., 1974; Bès and Broglia, 1975; Bès et al., 1976a,b,c; Mottelson, 1976; Broglia et al., 1976; Bès and Broglia, 1977; P. F. Bortignon et al., 1977; Bès and Kurchan, 1990). With the help of these modified formfactors (cf. also Vaagen et al. (1979); Bang et al. (1980); Hamamoto (1970) and refs. therein), and of global optical potentials, one can calculate the absolute differential cross sections, quantities which can be directly compared with the experimental findings.

P. G. Reinhardt

calculate consistently

In this way one avoids to introduce, let alone use spectroscopic factors, quantities which are rather elusive to define (cf. Duguet and Hagen (2012); Jenning (2011); Dickhoff and Barbieri (2004), and refs. therein). This is in keeping with the fact that as a nucleon moves through the nucleus it feels the presence of the other nucleons whose configurations change as time proceeds. It takes time for this information to be fed back on the nucleon. This renders the average potential nonlocal in time (cf. C. Mahaux et al. (1985) and references therein). A time–dependent operator can always be transformed into an energy dependent operator, implying an ω–dependence of the properties which are usually adscribed to particles like (effective) mass, charge, etc. Furthermore, due to Pauli principle, the average potential is also non local in space (cf. Apps 6.A and 6.B) Consequently, one is forced to deal with nucleons which carry around a cloud of (quasi) bosons,

[1] It is of notice that single–particle modified formfactors have their counterpart in the renormalised transition densities (Ch. 5 (inelastic scattering)) and in the modified two–nucleon transfer formfactors (Chapter 7, Eqs. (7.2.48; simultaneous), (7.2.135–7.2.136; successive) and (7.2.155–7.2.156; non–orthogonality) associated with inelastic and with pair transfer reactions (cf. Broglia et al. (1973); Potel et al. (2013) and refs. therein), respectively (cf. App. 6.H).

aside from exchanging its position with that of the other nucleons. It is of notice that the above mentioned phenomena are not only found in nuclear physics, but are common within the framework of many–body systems as well as of field theories like quantum electrodynamic (QED). In fact, a basic result of such theories is that nothing is really free (Feynman, 1975). A textbook example is provided by the Lamb shift, resulting from the dressing of the hydrogen atom electron, as a result of the exchange of this electron with those participating in the spontaneous, virtual excitation (zero point fluctuations (ZPF)) of the QED vacuum (cf. Apps 6.C, 6.D and 6.E). Within this context see Sect. 6.2 (Examples and Applications) concerning the phenomenon of parity inversion in the N=6 (closed shell) of exotic halo nuclei.

6.1 General derivation

We now proceed to derive the transition amplitude for the reaction (cf. Fig. 6.1.1).

$$A + a(= b + 1) \longrightarrow B(= A + 1) + b. \tag{6.1.1}$$

For a simplified version we refer to App 6.F, while for an alternative derivation within the framework of one–particle knock–out reactions we refer to App 6.G. Let us assume that the nucleon bound initially to the core b is in a single–particle state with orbital and total angular momentum l_i and j_i respectively, and that the nucleon in the final state (bound to core A) is in the l_f, j_f state. The total spin and magnetic quantum numbers of nuclei A, a, B, b are $\{J_A, M_A\}, \{J_a, M_a\}, \{J_B, M_B\}, \{J_b, M_b\}$ respectively. Denoting ξ_A and ξ_b the intrinsic coordinates of the wavefunctions describing the structure of nuclei A and b respectively, and $\mathbf{r}_{An}$ and $\mathbf{r}_{bn}$ the relative coordinates of the transferred nucleon with respect to the CM of nuclei A and b respectively, one can write the "intrinsic" wavefunctions of the colliding nuclei A, a as

$$\begin{aligned} &\phi^{J_A}_{M_A}(\xi_A), \\ &\Psi(\xi_b, \mathbf{r}_{b1}) = \sum_{m_i} \langle J_b\ j_i\ M_b\ m_i | J_a\ M_a \rangle \phi^{J_b}_{M_b}(\xi_b) \psi^{j_i}_{m_i}(\mathbf{r}_{bn}, \sigma), \end{aligned} \tag{6.1.2}$$

while the "intrinsic" wavefunctions describing the structure of nuclei B and b are

$$\begin{aligned} &\phi^{J_b}_{M_b}(\xi_b), \\ &\Psi(\xi_A, \mathbf{r}_{A1}) = \sum_{m_f} \langle J_A\ j_f\ M_A\ m_f | J_B\ M_B \rangle \phi^{J_A}_{M_A}(\xi_A) \psi^{j_f}_{m_f}(\mathbf{r}_{An}, \sigma). \end{aligned} \tag{6.1.3}$$

For an unpolarized incident beam (sum over M_A, M_a and divide by $(2J_A+1), (2J_a+1)$), and assuming that one does not detect the final polarization (sum over M_B, M_b),

(for details in the notation we refer to Figs. 7.C.1 and 7.C.2 and to the last paragraph before Sect. 7.C.1 of App. 7)

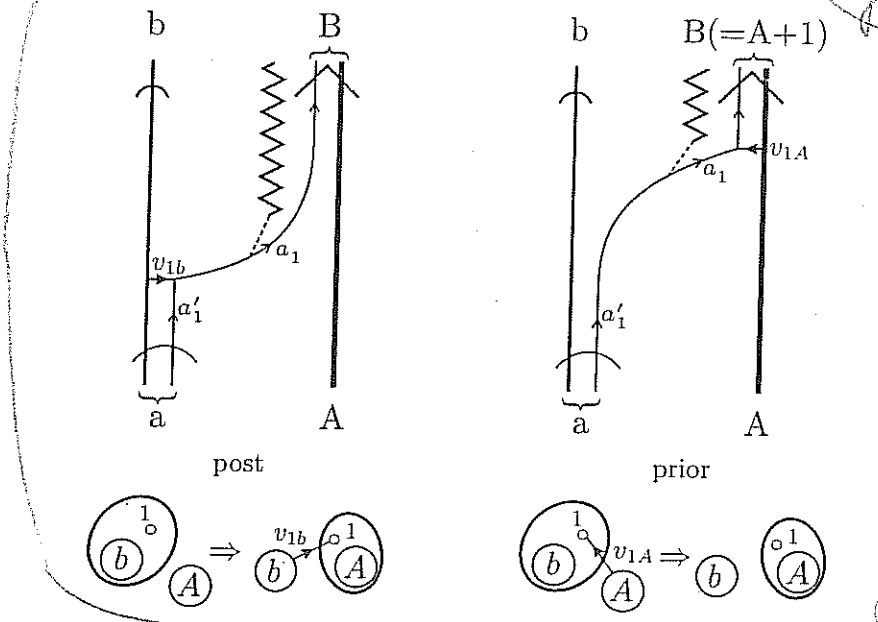

transfer

Figure 6.1.1: NFT graphical representation of the one–particle reaction $a(= b + 1) + A \rightarrow b + B(= A + 1)$. The time arrow is assumed to point upwards. The quantum numbers characterizing the states in which the transferred nucleon moves in projectile and target are denoted a'_1 and a_1 respectively. The interaction inducing the nucleon to be transferred can act either in the entrance channel ((a, A); v_{1A}, prior representation) or in the exit channel ((b, B); v_{1b}, post representation), in keeping with energy conservation. In the transfer process, the nucleon changes orbital at the same time that a change in the mass partition takes place. The corresponding relative motion mismatch is known as the recoil process, and is represented by a jagged line which provides information on the evolution of r_{1A} (r_{1b}). In other words, on the coupling between ~~reaction and transfer modes~~ structure and reaction (relative motion) degrees of freedom.

6.1.2 Zero–range approximation

In the zero range approximation,

$$\int dr_{bn} r_{bn}^2 u_{j_i}(r_{bn}) V(r_{bn}) = D_0; \quad u_{j_i}(r_{bn}) V(r_{bn}) = \delta(r_{bn})/r_{bn}^2. \tag{6.1.33}$$

It can be shown (see Fig. 6.1.2) that for $r_{bn} = 0$

$$\mathbf{r}_{An} = \frac{m_A + 1}{m_A}\mathbf{r}_f, \quad \mathbf{r}_i = \frac{m_A + 1}{m_A}\mathbf{r}_f. \tag{6.1.34}$$

One then obtains

$$t_{ll'}^K = \frac{-16\sqrt{2}\pi^2}{k_f k_i}(-1)^K \frac{D_0}{\alpha} i^{l'-l} e^{\sigma_f^l + \sigma_i^{l'}} \frac{\sqrt{(2l+1)(2l'+1)(2l_i+1)(2l_f+1)}}{2K+1} ((l_f \tfrac{1}{2})_{j_f}(l_i \tfrac{1}{2})_{j_i} | (l_f l_i)_K (\tfrac{1}{2}\tfrac{1}{2})_0)_K$$
$$\times \langle l\, l'\, 0\, 0 | K\, 0\rangle \langle l_f\, l_i\, 0\, 0 | K\, 0\rangle \int dr_f\, f_l(r_f) g_{l'}(\alpha r_f) u_{j_f}(\alpha r_f), \tag{6.1.35}$$

with

$$\alpha = \frac{A+1}{A}. \tag{6.1.36}$$

6.2 Examples and Applications

In this section we discuss some examples which illustrate the workings of single–particle transfer processes at large and, in particular the flavour of the limitations by which nuclear structure studies suffer, when this specific probe to study quasi-particle properties is not operative. Let us in fact start with such an example.

6.2.1 Dressing of single–particle states: parity inversion in ^{11}Li

The $N = 6$ isotope of $^9_3$Li displays quite ordinary structural properties and can, at first glance, be thought of a two-neutron hole system in the $N = 8$ closed shell. That this is not the case emerges clearly from the fact that ^{10}Li is not bound. Furthermore, the fact that the two lowest unoccupied states are the virtual $(1/2^+)$ and the resonant $(1/2^-)$ states, testify to the fact that, in the present case, the $N = 6$ is a far better magic neutron number than $N = 8$. Furthermore, the fact that the unbound $s_{1/2}$ state lies lower than the unbound $p_{1/2}$ state, a phenomenon known in the literature as parity inversion (see below), is in plain contradiction with static mean field theory. Dressing the (standard) mean field (e.g. Saxon–Woods potential, cf. Bohr and Mottelson (1969) Eqs. (2–181)–(2–182)) single-particle states with vibrations of the ^{9}Li core in terms of polarization (effective mass-like) and correlation (vacuum zero point fluctuations (ZPF)) diagrams, similar to those associated with the (lowest order) Lamb shift Feynman diagrams, (cf. App 6.D), shifts

In addition, the observation that

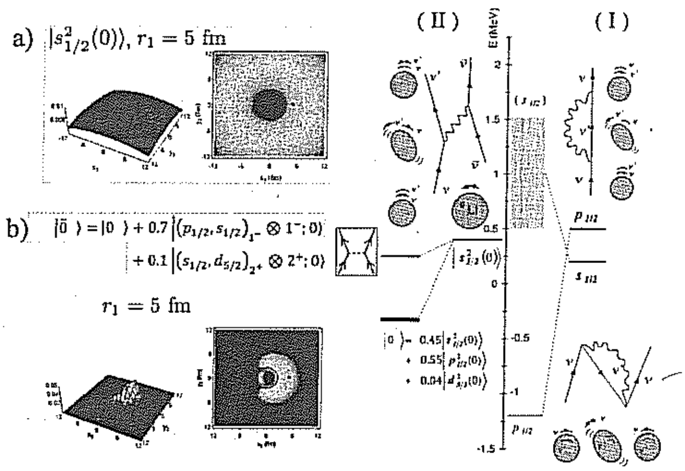

Figure 6.1.3: (I) NFT self-energy processes, giving rise to parity inversion in ^{10}Li; (II) bare (boxed inset) and induced pairing interaction binding the halo neutron pair to the ^{8}He core, through a bootstrap mechanism, in which the neutrons exchange the pigmy dipole resonance of ^{11}Li, as well as the quadrupole vibration of the core, as testified by the wavefunction b). The color snapshots displayed in a) and b) attempt at describing the becoming of the neutron halo Cooper pair of ^{11}Li, from an uncorrelated $s^2_{1/2}(0)$ configuration to a strongly correlated, (weakly) bound two-neutron state. It is of notice that the bare interaction (boxed inset in (II)), lowers the $s^2_{1/2}(0)$ (as well as the $p^2_{1/2}(0)$) pure configurations by only 100 keV, and is not able, by itself, to bind the pair. The color plots display the modulus square of the two-neutron wavefunction as a function of the coordinates of the two nucleons (left) and the probability distribution of one neutron with respect to the second one held fixed on the x-axis (at a radius of 5fm, solid dot). The red circle schematically represents the core. After F. Barranco et al. (2001).

Fig. 6.1.3 (II)

, nor to give rise to any significant mixing between these two configurations.

to text p. 25

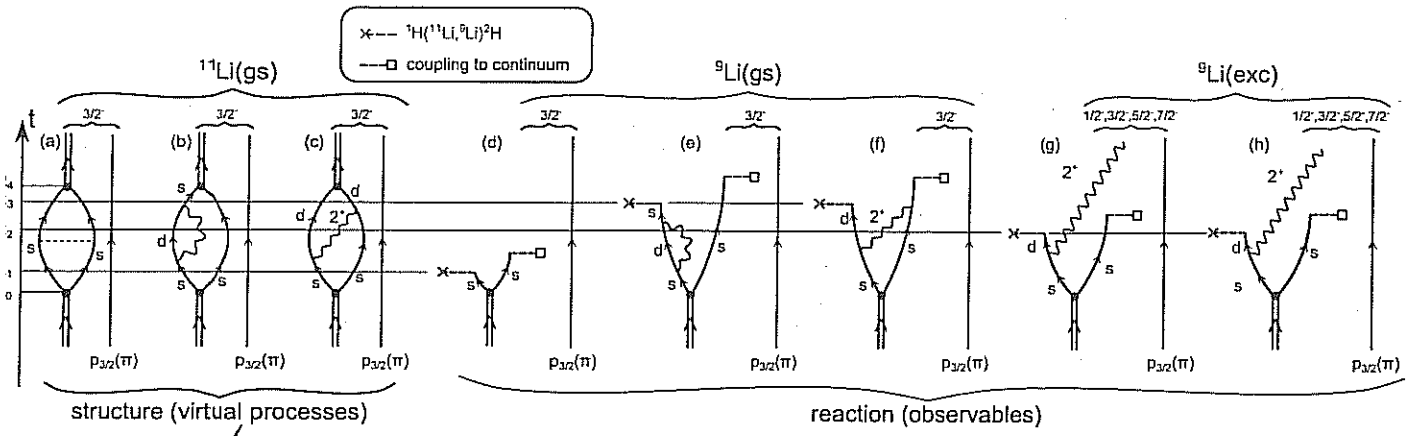

Figure 6.1.4: Nuclear Field Theory diagrams describing the basic, lowest order processes, by which the di-neutron halo binds to the $^9_3Li_6$ core (**structure**), and those associated with a one-neutron pick–up process (**reaction**).

the $s_{1/2}$ and $p_{1/2}$ mean field levels around. In particular the $p_{1/2}$ from a bound state (≈ -1.2MeV) to a resonant state lying at ≈ 0.5 MeV (Pauli principle, vacuum ZPF process), the $s_{1/2}$ being lowered and becoming a virtual state (≈ 0.2 MeV).

How can one check that CO and PO like processes as the ones shown in Fig. 6.1.3 (I) (cf. also Fig. 6.B.1) are the basic processes dressing the odd neutron of ^{10}Li, and thus the mechanism at the basis of parity inversion? The answer is, forcing these virtual processes to become real. In other words, act on the system with an external field so that certain off–the–energy shell states become on–the–energy shell. In fact a reaction like ^{1}H(^{11}Li,^{9}Li)^{2}H can populate single–particle states in ^{10}Li, in particular the two lowest states of ^{10}Li, namely the virtual and the resonant $|s_{1/2}\rangle$ and $|p_{1/2}\rangle$ states respectively. Being these states embedded in the continuum the system will eventually decay into both the ground and excited states of ^{9}Li (cf. Fig. 6.1.4). Now, similar indirect information can be obtained with the help of two–particle transfer processes, namely that associated with inverse kinematics (p,t) reaction (I. Tanihata et al., 2008), ^{1}H(^{11}Li,^{9}Li(2.69MeV; $1/2^-$))^{3}H (cf. Fig. 6.1.5 and Chs. 7 and 8 Sects. 7.2.10 and 8.2.3). Such a reaction is feasible and has been studied (I. Tanihata et al., 2008), in keeping with the fact that, adding a neutron to ^{10}Li leads to a bound state (see Fig. 6.1.3 (II)). In fact, $^{11}_3$Li$_8$ displays a two–neutron separation energy $S_{2n} \approx 400$ keV (for further details we refer to Ch. 8, Sect. 8.2.3). A price to pay for not being able to use the specific probe for single–particle modes (one–particle transfer), is that of adding to the self–energy contributions in question those corresponding to vertex corrections (for details cf. App 6.E, Figs 6.E.1 and 6.E.2 and Ch. 8 Sect. 8.2.3 (application $2n$–transfer)).

Within the present context, it is difficult if not impossible to talk about single–particle motion without also referring to collective vibrational states (cf. e.g. Fig. 6.1.3 (II)), or to talk about pair addition and pair substraction correlations, without

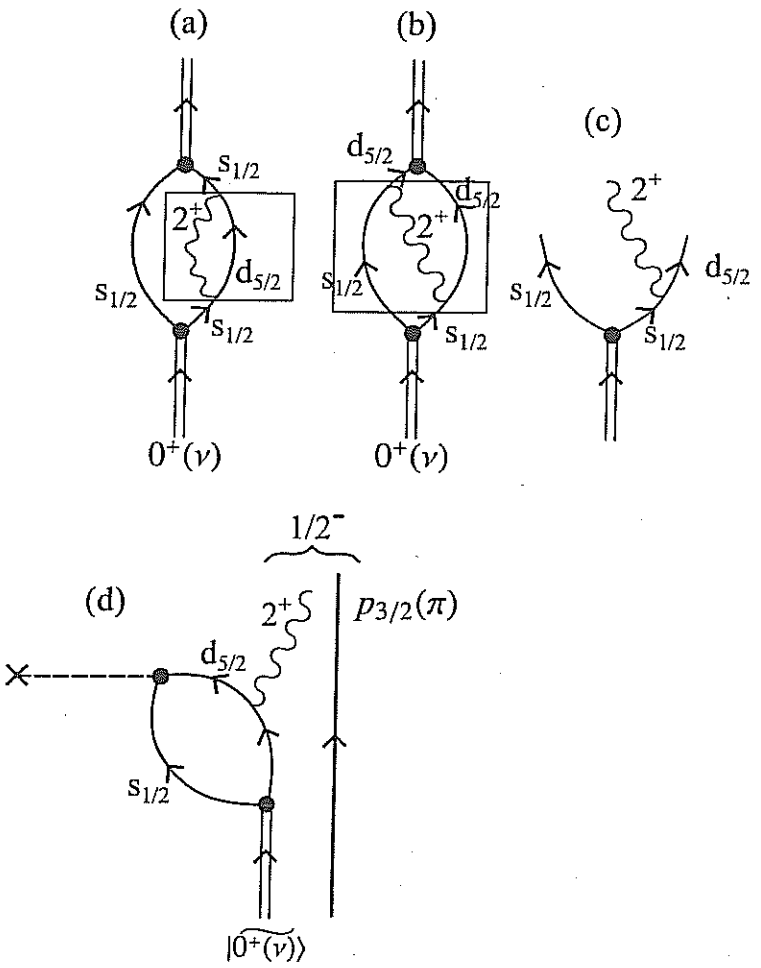

Figure 6.1.5: (a) Self–energy (see boxed process) and (b) vertex (pairing induced interaction) renormalization process, both associate with (c) a (two–particle)–(quadrupole vibration) intermediate (virtual state) which can be forced to became real in a (p,t) reaction ^{1}H(^{11}Li,^{9}Li)^{3}H exciting the first excited state $|2.69\text{MeV};1/2^-\rangle$ of ^{9}Li (see Ch.8).

at the same time talking about correlated particle–hole (e.g. density) vibrations and dressed quasiparticle motion (see e.g. Fig. 6.1.5 (a) and (b)), again concerning both structure and reactions. Within the framework of the present monograph, the above facts imply that Chapters 5 (inelastic), 6 (one–particle transfer) 7 and 8 (two–particle transfer and applications) form a higher unity. This unity extends also to the content of App 6.G (knock–out reactions), as well as to the question of inelastic channels and of final state interactions, and thus of the possibility that the population of the excited state $1/2^-$ depicted in Fig. 6.1.5 (d) receives contributions other, and more involved, than those associated with the direct two–nucleon pick–up depicted (for details cf. Ch. 8, in particular App. 8.B, Table 8.B.1; cf. also (Potel et al., 2010)).

Let us now return to the discussion of the one–particle transfer process ^{1}H(^{11}Li,^{9}Li)^{3}H, that is the pickup of a neutron from the pair addition halo state $|^{11}\text{Li(gs)}\rangle$ (cf. Fig. 6.1.4). In keeping with the fact that ^{10}Li is not bound, such a reaction populates only transiently the virtual and resonant states of ^{10}Li and eventually, after the second neutron of the pair spoliated of its dynamical glue leaves the system by going into the continuum, a state in ^{9}Li is populated (cf. Figs. 6.1.4 (d)–(f) and 6.1.4 (g) and (h)). In drawing the different NFT diagrams time **t** is assumed to run upwards. External fields and the bare NN–interaction are assumed to act instantaneously, while the couplings to the phonon modes (wavy lines) lead to retarded (ω–dependent) effects. For simplicity, only the quadrupole vibrational mode of the ^{8}He core is considered, as well as only the virtual s- and continuum d- single-particle states are taken into account. The halo Cooper pair (pair addition mode of the $N = 6$ closed shell system) carries angular momentum 0^+ and is represented by a double arrowed line, the odd proton (π) which occupies a $p_{3/2}$ state, is represented by a single arrowed line and is here treated as a spectator. The di-neutron system binds to the core through (**a**) the bare interaction (horizontal dashed line) acting between the two-neutron, each represented by a single arrowed line, and through the renormalizing process associated with the coupling of the neutrons with a variety of modes (cf. Fig. 6.1.3) of which we select as example, the quadrupole vibration of the ^{8}He; (**b**) effective mass processes associated with the quadrupole vibration of ^{8}He (wavy line) renormalizing the energy of the $s_{1/2}$ continuum state and leading to an almost bound (virtual) state ($\approx$ 0.2 MeV). (**c**) Induced pairing interaction associated with the quadrupole vibration of ^{8}He. (**d**) Intervening the process (a) at any time after $\mathbf{t}_0$ and before $\mathbf{t}_4$ with an external single-neutron pick-up field (cross followed by an horizontal dashed line), and processes (b) and (c) at $\mathbf{t}_0 < \mathbf{t} < \mathbf{t}_1$, leads to the ground state of ^{9}Li, in keeping with the fact that the second neutron will leave the system almost immediately, ^{10}Li not being stable. (**e**) Same as above but in connection with process (b) and now after the nucleon has reabsorbed the quadrupole phonon and before $\mathbf{t}_4$, i.e. acting at $\mathbf{t}_3 < \mathbf{t} < \mathbf{t}_4$ leads again to the population of the ^{9}Li ground state. (**f**) same as (e) but in this case the external field acts on the process (c). Let us now consider the one-nucleon pickup processes populating the $(2 \otimes p_{3/2}(\pi))_{J^\pi}$, ($J^\pi = 1/2^-, 3/2^-, 5/2^-$ and $7/2^-$) multiplet of ^{9}Li, in particular the lowest $|1/2^-; 2.69\,\text{MeV}\rangle$ state. In this case the

external field has to act at a time t_2 on (b) and on (c) leading to the (identical final states displayed in (g) and on (h) (Fig. 6.1.4). While the single contribution associated with mass renormalization process ((b)→(g)) and vertex corrections ((c)→(h)) cannot be distinguished experimentally, one can estimate the relative contribution to the corresponding absolute cross section. The wavefunction of F. Barranco et al. (2001) (cf. also Fig. 6.1.3 (b) and (II)) predict a ratio 3/1 (**Ricardo checks**).

Before concluding the present section, and in connection with Figs. 6.1.4 (g,h) and 6.1.5 (d), it may be useful to remind us what, within the framework of quantum mechanics, one can learn from a reaction experiment. It is not "what is the state after the collision" but "how probable is a given effect of the collision". Within this context: "The motion of particles follows probability laws, but the probability itself propagates according to the laws of causality" (Born, 1926)[2].

6.2.2 ^{132}Sn(d,p)^{133}Sn and ^{132}Sn(p,d)^{131}Sn reactions

6.2.3 ^{120}Sn(d,p)^{121}Sn and ^{120}Sn(p,d)^{119}Sn reactions

Appendix 6.A Minimal requirements for a consistent mean field theory

In what follows the question of why, rigorously speaking, one cannot talk about single–particle motion, let alone spectroscopic factors, not even within the framework of Hartree–Fock theory, is briefly touched upon.

As can be seen from Fig. 6.A.1 the minimum requirements of selfconsistency to be imposed upon single–particle motion requires both non–locality in space (HF) and in time (TDHF)

$$i\hbar\frac{\partial\varphi_\nu}{\partial t} = -\frac{\hbar^2}{2m}\nabla^2\varphi_\nu(x,t) + \int dx'dt' U(x-x', t-t')\varphi_\nu(x',t'), \qquad (6.A.1)$$

[2] If there is a lesson to be learned from the above discussion is the fact that, in dealing with a specific feature of a quantal many–body system, e.g. single–particle motion in nuclei (structure) and one–particle transfer process (reaction), one can hardly avoid to talk about other elementary modes of excitation and reaction channels, respectively. Within the scenario of the chosen example, this is because a nucleon which, in first approximation is in a mean field stationary state, can actually be viewed as a fermion moving through a gas of ephimerous $2p-2h$ composite virtual excitations, that is $(p-h)$ + density and/or $2h(2p)$ + pair addition (substraction) excitations, arising from vacuum (ground state) ZPF and giving rise to the nuclear vacuum ω–dependent dielectric function. Because of Pauli principle (Pauli, 1947) the nucleon in question is forced to exchange role with the virtual, off–the–energy–shell nucleons, thus leading to CO processes (cf. Fig. 6.B.1 (b)) and eventually, through time ordering, to PO ones (cf. Fig. 6.B.1 (a)). Such processes, eventually carried out to high order in the nucleon–vibration coupling, eventually diagonalize the nuclear Hamiltonian, taking care of the overcompleteness (non–orthogonality) and of Pauli violations of the basis made out of elementary modes of nuclear excitation, thus leading to dressed (observable) modes, single–particle states in the present case, whose properties, e.g. absolute single–particle transfer cross sections, can be compared with the data without further ado, ~~provided the different reaction channels, e.g. inelastic ones, are properly considered.~~

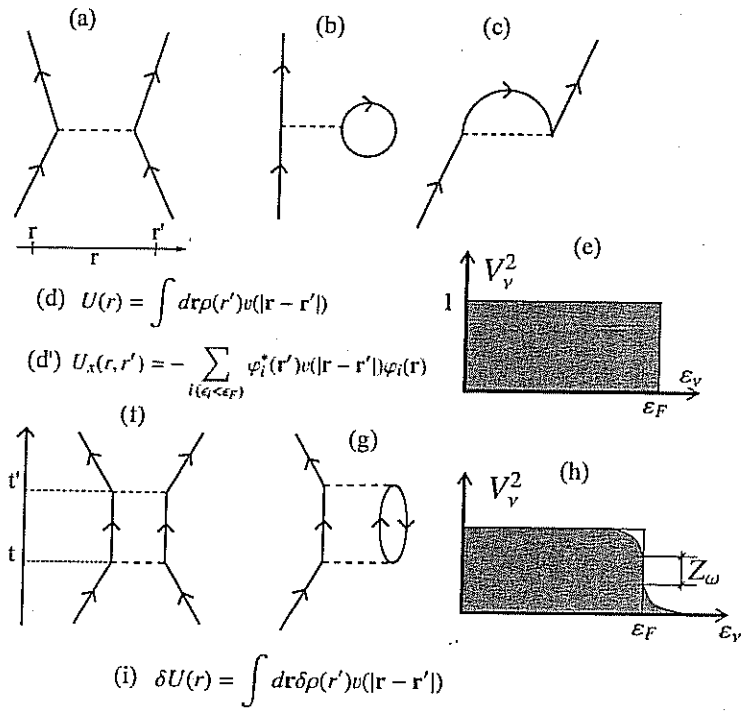

Figure 6.A.1: (a)Scattering of two nucleons through the bare NN interaction $v|\mathbf{r}-\mathbf{r}'|$, (b) contribution to the direct (U, Hartree) and (c) to the exchange (U_x, Fock) potential, resulting in (d) the (static) self–consistent relation between potential and density (non–local (d')), which (e) uncouples occupied ($\varepsilon_\nu \leq \varepsilon_F$) from empty states ($\varepsilon_\nu > \varepsilon_F$), (f) multiple scattering of two nucleons lead, through processes like the one depicted in (g), eventually propagated to all orders, to: (h) softening of the discontinuity of the occupancy of levels at ε_F, as well as to: (i) generalization of the static selfconsistency into a dynamic relation encompassing also collective vibrations (Time–dependent HF solutions of the nuclear Hamiltonian, conserving energy weighted sum rules (EWSR).

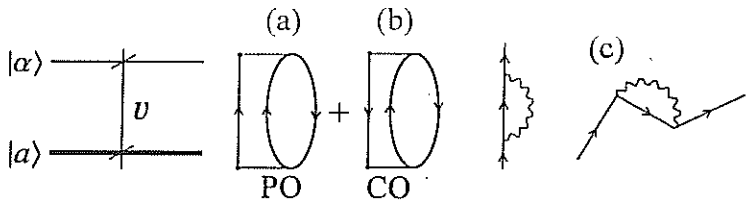

Figure 6.B.1: Two state schematic model describing the breaking of the strength of the pure single–particle state $|a\rangle$, through the coupling to collective vibrations (wavy line) associated with polarization (PO) and correlation (CO) processes.

H^{KS} being known as the Kohn–Sham Hamiltonian, $V_{ext}(\mathbf{r})$ being the field created by the ions and acting on the electrons. Both the Hartree and the exchange–correlation potentials $U_H(\mathbf{r})$ and $U_{xc}(\mathbf{r})$ depend on the (local) density, hence on the whole set of wavefunctions $\varphi_\gamma(\mathbf{r})$. Thus, the set of KS–equations must be solved selfconsistently (cf. e.g. (Broglia et al., 2004) and refs. therein).

Appendix 6.B Model for single–particle strength function: Dyson equation

In the previous section we introduced the argument concerning the impossibility of defining a "bona fide" single–particle spectroscopic factor. It was done with the help of Feynman (NFT) diagrams. In what follows we essentially repeat the arguments, but this time in terms of Dyson's (Schwinger) language. For simplicity, we consider a two–level model where the pure single–particle state $|a\rangle$ couples to a more complicated state $|\alpha\rangle$, made out of a fermion (particle or hole), coupled to a particle–hole excitation which, if iterated to all orders can give rise to a collective state (cf. Fig.6.B.1). The Hamiltonian describing the system is

$$H = H_0 + v, \tag{6.B.1}$$

where

$$H_0|a\rangle = E_a|a\rangle, \tag{6.B.2}$$

and

$$H_0|\alpha\rangle = E_\alpha|\alpha\rangle. \tag{6.B.3}$$

Let us call $\langle a|v|\alpha\rangle = v_{a\alpha}$ and assume $\langle a|v|a\rangle = \langle\alpha|v|\alpha\rangle = 0$.

From the secular equation

$$\begin{pmatrix} E_\alpha & v_{a\alpha} \\ v_{a\alpha} & E_a - E_i \end{pmatrix} \begin{pmatrix} C_\alpha(i) \\ C_a(i) \end{pmatrix} = 0, \tag{6.B.4}$$

and associated normalization condition

$$C_a^2(i) + C_\alpha^2(i) = 0, \tag{6.B.5}$$

one obtains

$$C_a^2(i) = \left(1 + \frac{v_{a\alpha}^2}{(E_\alpha - E_i)^2}\right)^{-1}, \tag{6.B.6}$$

and

$$\Delta E_a(E) = E_a - E = \frac{v_{a\alpha}^2}{E_a - E}. \tag{6.B.7}$$

The energy of the correlated state

$$|\tilde{a}\rangle = C_a(i)|a\rangle + C_\alpha(i)|\alpha\rangle, \tag{6.B.8}$$

is obtained by the (iterative) solution of the Dyson equation (6.B.7), which propagate the bubble diagrams shown in Figs 6.B.1 (a) and (b) to infinite order leading to collective vibrations (see Fig. 6.B.1 (c)).

With the help of the definition given in eq (6.A.5), and making use of the fact that in the present case, the quantity U appearing in this equation coincides, within th present context with $\Delta E_a(E)$, one obtains that the discontinuity of the single–particle levels at the Fermi energy is given by

$$Z_\omega = C_a^2(i) = \left(\frac{m_\omega}{m}\right)^{-1}. \tag{6.B.9}$$

Making use of the solution of the Dyson equation (6.B.7), and of the relations (6.B.5) and (6.B.6), one can calculate the renormalized state $|\tilde{a}\rangle$ (Eq. 6.B.8) to be employed in working on the associated modified, single–particle transfer form factor to be used in the calculation of the absolute value of one–particle transfer cross sections (cf. e.g. Sects. 6.2.2 and 6.2.3, where the application of the above concepts and techniques is applied to the study of one–neutron transfer reactions in open shell, superfluid (^{120}Sn) and in closed shell (^{132}Sn) nuclei).

Appendix 6.C Antiparticles: proof of concept of the quantal vacuum and of medium polarization effects

Let us consider a massive quantal particle, e.g., an electron, which moves at a velocity close of that of light. Because of Heisenberg relations, there exists a finite possibility to observe the particle moving at a velocity larger than its average velocity, and thus faster than light, a possibility ruled out by special relativity. The only way to avoid this, is by introducing antiparticles, that is a hole in the "vacuum" filled to the rim (Fermi energy) with particles, thus providing the physics to the negative energy solutions of Dirac equation.

In other words, when an electron approaches the maximum speed with which information propagate in a medium, like e.g. in the case of an electron the QED vacuum, processes like the one depicted in Fig. 6.C.1 become operative. In other